RESEARCH ARTICLE

Screening of Novel Inhibitors Targeting the Non-ATP-binding Domain of *Staphylococcus aureus* SecA1

Yan Liu¹, Qing Su¹, Zonglin Wang¹, Peiyao Liu¹, Jinjin Hong¹, Hyuk-kyu Seoh², Xu Jia³, Sen-Fang Sui⁴, Phang-Cheng Tai^{2,*} and Xinhe Huang^{1,*}

¹School of Life Science and Engineering, Southwest Jiaotong University, Chengdu 610031, China; ²Department of Biology, Georgia State University, Atlanta, GA 30303, USA; ³Non-coding RNA and Drug Discovery Key Laboratory of Sichuan Province, Chengdu Medical College, Chengdu, Chengdu 610599, China; ⁴State Key Laboratory of Membrane Biology, Center for Structural Biology, School of Life Sciences, Tsinghua University, Beijing 100084, China

Abstract: *Objective*: *Staphylococcus aureus* (*S. aureus*) has been one of the pathogenic bacteria for clinical infections, and there is an urgent need for the development of novel anti-*S. aureus* drugs. SecA is a conserved and essential protein in bacteria and is considered as an ideal target for development. Current screening of inhibitors against SecA has focused on the ATP-binding structural domain, which increases the risk of drug side effects, so a novel screening strategy based on the non-ATP-binding structural domain was chosen in this paper.

Methods: A three-dimensional structural model of *S. aureus* SecA1N75 was constructed, and molecular docking was utilized to screen small molecules with strong interactions with the non-ATP binding domains from a compound library, and four candidate compounds were finally targeted. Molecular dynamics simulations of the candidate molecules were performed to evaluate their drug potential.

Results: The four candidate compounds formed stable interactions with key residues of the SecA binding pocket. Molecular dynamics simulations further showed that the candidate molecules bound to the receptor in a stable conformation with nM-level inhibition constants, displaying potent SecA inhibitory activity. It lays the foundation of a lead compound for the development of antimicrobial drugs targeting SecA.

Conclusion: In this thesis, an inhibitor screening strategy based on non-ATP binding structural domains was successfully constructed, which breaks through the limitations of traditional methods to screen candidate molecules with high activity and low risk of potential side effects, and provides an innovative solution to meet the challenge of *S. aureus* drug resistance.

Keywords: *Staphylococcus aureus*, SecA1 Inhibitors, Virtual Screening, Non-ATP binding domains, Molecular Docking, Molecular Dynamics (Gromacs).

ARTICLE HISTORY

Received: November 30, 2024 Revised: February 08, 2025 Accepted: February 20, 2025

DOI: 10.2174/0115734064370398250426162503

1. INTRODUCTION

S. aureus belongs to the genus Staphylococcus and is a representative of Gram-positive pathogenic bacteria [1]. S. aureus becomes the third most important microbial pathogen, along with Salmonella and Parahaemolyticus [2]. Its causative agent, enterotoxin, is a single-chain, small secretory protein with molecular weight of about 26-29 kDa, relatively low molecular mass, and thermal stability [3]. It causes damage to the human gut and lead to symptoms such as vomiting and diarrhea [4].

School of Life Science and Engineering, Southwest Jiaotong University, Chengdu 610031, China; E-mail: Xinhehuang@swjtu.edu.cn

Due to the widespread increase in antibiotic resistance in *S. aureus*, methicillin-resistant *Staphylococcus aureus* (MRSA) and methicillin-sensitive *Staphylococcus aureus* (MSSA) are common drug-resistant strains in clinical settings [5]. MRSA infections result in higher mortality, morbidity, and longer hospital stays compared to MSSA infections [6]. Some MSSA lineages, such as certain sequence types (ST), may have high virulence and cause severe infections [7]. With the growing issue of antibiotic resistance and rapid changes in epidemiology, there is an urgent need for new treatment strategies [8].

SecA, a crucial protein involved in protein secretion, exists in both soluble and membrane-bound forms within bacterial cells [9, 10]. It is highly conserved across bacterial species, and because it is absent in mammalian cells, inhibitors targeting SecA present a reduced risk of side effects in

^{*}Address correspondence to these authors at the Department of Biology, Georgia State University, Atlanta, GA 30303, USA; E-mail: Biopct@gsu.edu

humans [11, 12]. The Sec pathway plays a vital role in cellular protein transport, particularly in the secretion of toxins. SecA is the main energy-converting enzyme in this pathway [13, 14], which utilizes the energy from ATP hydrolysis to facilitate transmembrane transport of precursor proteins [15, 16]. In some pathogenic Gram-positive bacteria like S. aureus, the SecA analog is SecA1, and the soluble SecA2 works in conjunction with SecA1, participating in the secretion of proteins that are not transported via the Sec pathway [17, 18], as well as assisting in the secretion of specific pathogenic or protective factors. Since not all bacteria have SecA2, we chose SecA1, the analog of all bacteria, as the focus of our study [19]. Li et al. used the crystal structure of Escherichia coli SecA and found, for the first time, that two compounds had good inhibitory activity through virtual screening [20]. Structures of Candidatus Liberibacter asiaticus SecA were constructed by homology modelling by Akula [21] et al. and Zhang [9] et al. In addition to the structure-based virtual screening, SecA inhibitors have been isolated and extracted from fungi, such as the first natural product SecA inhibitor, equisetin (CJ-21058) [22], isolated from an unknown fungus. Azide was the first known SecA inhibitor, but it is a non-selective eukaryotic enzyme inhibitor and therefore not a useful antimicrobial agent [23]. Wang et al. used *Pseudomonas aeruginosa* for the development and application of a SecA ATPase inhibitor screening model, and the low uM SecA inhibitors had been found too [24]. In addition, three conformational types of SecA small molecule inhibitors were designed and evaluated in Tai and Wang's laboratories: Rose Bengal (RB) analogue [25, 26], 5-cyano-6-thiopyrimidine analogue [27] and triazole pyrimidine analogue [28]. Recently, we were able to successfully construct a crystal model of *Helicobacter pylori* SecA, and through virtual screening, identified a number of small-molecule potential inhibitors [10] that affect SecA ATPase and antibacterial activities. Although studies have reported inhibitors [10, 15, 29], the structure of S. aureus SecA and its inhibitors has not yet been analyzed.

Recent studies indicate that SecA can be an effective target for the development of novel antibacterial drugs [29] and that further optimization of compound potency and selectivity for SecA with minimal toxicity issues is warranted. The main issues at this stage of research on SecA inhibitors are the solubility of the drugs and the membrane permeability of the drug molecules, especially the outer membrane barrier of Gram-negative bacteria [30, 31]. The novel SecA inhibitors do not need to enter the cytoplasm and can bind the membrane-bound SecA directly [32, 33], with a lower impact on drug penetration and intracellular concentration [32, 34]. However, there is currently no screening of novel inhibitors targeting the SecA domain of S. aureus. Especially, we want to screen for the non-ATP-binding domain. Moreover, the previous virtual screenings of SecA were basically mostly based on the domains of ATP-binding structures, but there are many ATPase targets, whether in the human body or in bacteria, that the inhibitors targeting ATPases obtained in this way might have many side effects. Hu [7] et al. suggest that in addition to the ATP-binding orientation, there are two additional binding pockets in SecA molecules, NP1 and NP2, and that designing an insertion of deeper motifs (NP1 and NP2) to enhance the hydrophobic binding pockets of the small molecules could be an effective approach. Therefore, in this study, we targeted the pockets of SecA non-ATP-binding structural domains for virtual screening of potential candidates for the treatment of *S. aureus*. The C-terminal tail (CTT) of SecA affects the conformation of SecA [35, 36], disrupts effects on ribosome binding, substrate-protein binding, and ATPase activity. Therefore, we chose *S. aureus* SecA1 amino acids 1-707 as the model.

2. METHODS

2.1. Homology Modelling

The amino acid sequence from amino acids 1-707 of the analogous S. aureus SecA1 protein (Accession number: PZK95531) was accessed from the National Centre for Biotechnology Information Database (NCBI, https://www. ncbi.nlm.nih.gov/protein/), and used as a template protein for the BLAST search (https://blast.ncbi.nlm.nih.gov/Blast.cgi) to model the target. The homology model was generated with SWISS-MODEL [37] and energy minimization was performed using Swiss PDB viewer (SPDBV) 4.10 software. To evaluate the validity of the model, the binding sites from the template protein were removed and re-aligned to the binding sites of the homologous model. The root-meansquare deviation (RMSD) of the two conformations was compared. Finally, the models were evaluated by SAVES v6.0 (https://saves. mbi.ucla.edu/), which comprises protein structure evaluation tools such as ERRAT [38], VERIFY 3D [39], and PROCHECK [40].

2.2. Molecular docking

2.2.1. Construction of Small-molecule Ligands

These ligands were sourced from ZINC (https://zinc15.docking.org/), a total of 2,073 small molecules. The 2D structure of the molecule was then converted to 3D coordinates in the ionized state at pH 7.4 using Openbabel 2.4.1. Flexibility was assigned to all rotatable bonds in the ligands, and chirality was specified.

2.2.2. Coordination of Target Protein SecA1N75

The active site and docking pocket of the ligands were predicted using the DoGSite Scorer module from Proteins Plus (https://proteins.plus/). The selected pocket is located adjacent to and deeper than the ATP-binding site, with coordinates X: 58.683, Y: -23.824, Z: 19.692 (Å). The dimensions of the grid box were set to X: 16, Y: 13, Z: 20 (Å). Ligand docking for S. aureus SecA1N75 was carried out through High Throughput Virtual Screening (HTVS) and AutoDock Vina 1.2.2 for semi-flexible docking. The top 10 molecules were selected based on their high negative binding affinities for re-screening. In the second round, the highestscoring molecules were evaluated for binding interactions with the target using AutoDockTools 1.5.6 and AutoDock 4.2.6. This was followed by docking using the Lamarckian genetic algorithm (LGA) [41]. As in the first round, the docking search space was limited to the binding sites of S. aureus SecA1N75. The docking setup consisted of 55 runs per ligand, with a population size of 150, and the maximum number of generations and evaluations set at 27,000 and 25,000,000, respectively. After rescreening, select the topranked molecules and calculate the distance to the optimal complex with the highest negative binding affinity. For further analysis, the results were examined interactively using the PLIP server [42].

2.2.3. Molecular Dynamics Simulations (MD)

Before performing the MD simulations, both the molecular ligands and the S. aureus SecA1N75 protein need to be processed separately. First, the ACPYPE [43] server was used to assign a force field to the ligand and assemble the charge. The homology of the S. aureus SecA1N75 protein was then modelled using the generic AMBER99SB-ILDN force field [44]. Subsequently, the protein and ligand were assembled into a complex. All MD simulations were performed using the GROMACS 2021-GPU software package [45]. In each simulation, the complex was placed in a cubic box with a minimum distance of 1.0 nm between the protein and the box. The box was solvated using the classical TIP3P water model, and charge balanced with an appropriate amount of sodium ions (Na+). The system was gradually heated from 0 to 300 K using the NVT tethered equilibrium system for 100 ps, and then relaxed in the NPT tether for 200 ps. The system temperature was 300 K and the pressure was 1 atm. Finally, MD simulations were conducted under these conditions with a timestep of 2 fs for 50 ns. The data were saved on discs at 100 ps intervals for further analysis.

2.2.4. Binding Free Energy Calculations

The molecular mechanics Poisson-Boltzmann surface area method (MM-PBSA) was an efficient and popular method for calculating the free energy of binding of small ligands to biological macromolecules [46, 47]. In this study, the binding free energies of S. aureus SecA1N75 complexes were calculated using GROMACS tools. Taking into account of screening effects and conformational entropy (TDS), MM-PBSA calculations were performed using a modified shell script gmx mmpbsa [48].

2.2.5 ADME-T Properties

online server SwissADME-T [49] www.swissADME-T.ch) was used to predict the absorption, distribution, metabolism, and excretion of ADME-T. Prediction of compound toxicity was performed by using the AD-ME-TtSAR server (http://lmmd.ecust.edu.cn/ADME-Ttsar2/) [50].

3. RESULTS AND DISCUSSIONS

3.1 Homology Modelling

The template ray used is the X-ray crystal structure of Bacillus subtilis (B. subtilis) (PDB ID: 3jv2), the sequence identity and query coverage of SecA in B. subtilis was 63.18%, while in S. aureus it is 99%. In addition, the homology modeling structures of GMQE and QMEANDisCo [51] yielded SecA scores of 0.77 ± 0.05 and 0.80 in B. subtilis and S. aureus, respectively. Sequence comparisons were performed using ESPript 3.0 [52] (Fig. S1).

The stereo-chemical quality and accuracy of the predicted S. aureus SecA1N75 model was assessed using the SAVES v6.0 server, and the sequences of S. aureus SecA1N75 and S. aureus SecA2N75 were compared in Fig. S1. As shown in the Ramachandran plot, 95.1542% of S. aureus SecA1N75 residues were located in the "permissive region". Additionally, 93.0% of amino acids were in the most favorable region, 5.9% in the additional permissive region, 1.1% in the generously permissive region, and no amino acids were in the impermissive region. Furthermore, the ERRAT result was 95.154%, indicating high model resolution (Fig. S2). These results suggest that the overall conformation of the constructed S. aureus SecA1N75 model, including main chain and side chain stereochemistry, is suitable for subsequent virtual screening. The structure of the S. aureus SecA1N75 is depicted in Fig. 1 and was superimposed with the SecA template protein from B. subtilis (RMSD: 0.846 Å).

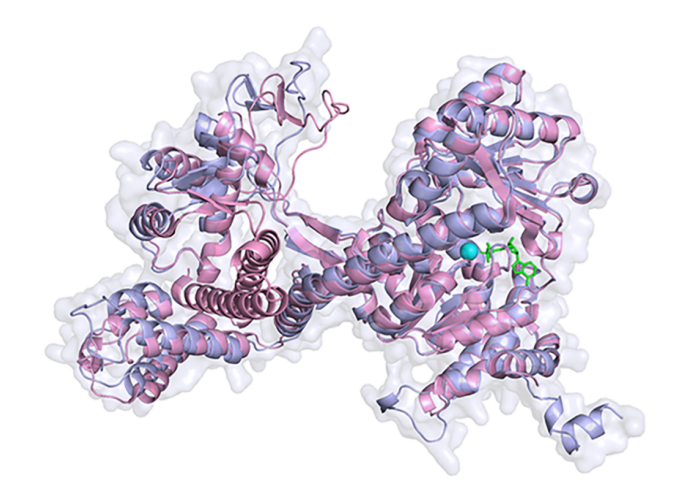


Fig. (1). Model of S. aureus SecA1N75 (purple) superimposed on the structure of B. subtilis SecA (pink) (PDB ID: 3jv2). ATP structure was shown as a rod (green). (A higher resolution / colour version of this figure is available in the electronic copy of the article).

3.2. Analysis of Molecular Docking and Binding Patterns

Molecular docking and binding pattern analysis were performed by using a semi-flexible docking method. A total of 2,073 small molecules were screened against S. aureus SecA1N75. The top 10 compounds with the lowest negative Vina scores, ranging from -9.9 to -10.5 kcal/mol. Subsequently, docking was repeated with AutoDock 4.2.6 to confirm the binding affinity, and the compounds were ranked accordingly. The results indicated that four of the ten ligands showed lower docking scores and were chosen for further analysis. These selected compounds were labeled as SW-569, SW-366, SW-849, and SW-2007. Table 1 presents a comparison of the binding affinities of these selected ligands with those of the control ligands for S. aureus SecA1N75. The interaction patterns of the four compounds with S. aureus SecA1N75 are depicted in Fig. 2.

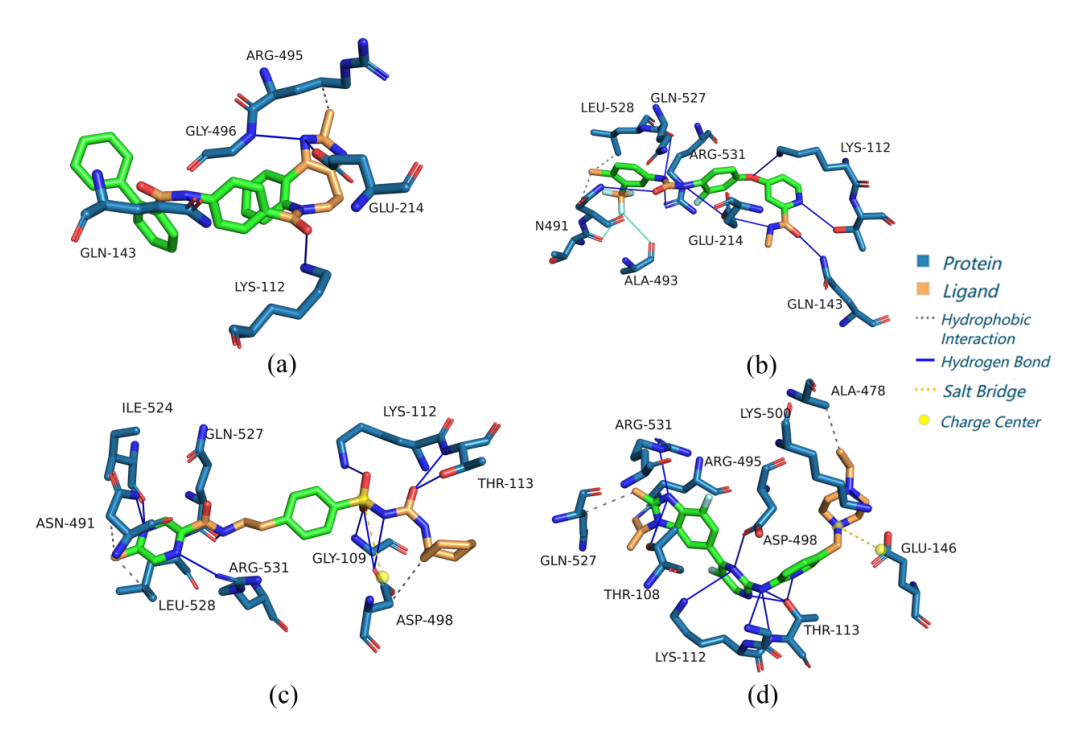


Fig. (2). Optimal ligands and control molecules for binding to *S. aureus* SecA1N75. These views are 3D representations of the *S. aureus* SecA1N75 substrate binding site residues interacting with (a) SW-569, (b) SW-366, (c) SW-849, (d) SW-2007. (*A higher resolution / colour version of this figure is available in the electronic copy of the article*).

Table 1. Comparison of AutoDock Vina binding affinity of selected ligands.

Com- pounds	Names	Molecular Formula	Molecular Weight (g/mol)	AutoDock Vina Bind- ing Affini- ty (kJ/mol)	AutoDock Inhibition Constant (nM)	Structure
SW-569	N-[4-(2-methyl-4,5-dihydro- 3H-imidazo[4,5- d]benzazepine-6- carbonyl)phenyl]-2- phenylbenzamide	с ₃₂ н ₂₆ N ₄ О ₂	498.6	-10.5	125.8	
SW-366	4-[4-[[4-chloro-3- (trifluorome- me- thyl)phenyl]carbamoylamino]- 3-fluorophenoxy]-N- methylpyridine-2-carboxamide	C ₂₁ H ₁₅ N ₄ O ₃ F ₄ Cl	482.8	-10.2	4.35×10 ⁻⁵	E H H H H H H H H H H H H H H H H H H H
SW-849	N-[2-[4- (cyclohexylcarbamoylsul- famoyl)phenyl]ethyl]-5- methylpyrazine-2-carboxamide	C21H27N5O4S	445.5	-10.4	24.37	
SW-2007	N-[5-[(4-ethylpiperazin-1-yl)methyl]pyridin-2-yl]-5-fluoro-4-(7-fluoro-2-methyl-3-propan-2-ylbenzimidazol-5-yl)pyrimidin-2-amine	C ₂₇ H ₃₂ F ₂ N ₈	506.6	-10.2	3.56×10 ⁻⁷	N N N N N N N N N N N N N N N N N N N

Compound SW-569 exhibits a binding affinity of -10.5 kJ/mol with SecA, with an inhibition constant of 125.8 nM. Docking results show that the ligand forms four hydrogen bonds with residues Lys112, Gln143, Glu214, and Gly496, and engages in hydrophobic interactions with Arg495, which stabilize the binding. Compound SW-366 has a binding affinity of -10.2 kJ/mol with SecA and an inhibition constant of 4.35×10-5 nM. Docking results indicate that the ligand forms eight hydrogen bonds with residues Lys112, Gln143, Glu214, Asn491, Gln527, and Arg531. Additionally, hydrophobic interactions with Asn491 and Leu58 further stabilize the binding. Compound SW-849 shows a binding affinity of -10.4 kJ/mol with SecA and an inhibition constant of 24.37 nM. Docking results reveal that the ligand forms ten hydrogen bonds with residues Gly109, Lys112, Thr113, Asn491, Asp498, Ile524, Gln527, and Arg531. Hydrophobic interactions with Asn491 and Leu528 also contribute to the stability of the binding. Compound SW-2007 has a binding affinity of -10.2 kJ/mol with SecA, with an inhibition constant of 3.56×10-7 nM. Docking results show that the ligand forms ten hydrogen bonds with residues Thr108, Lys112, Thr113, Asp498, Lys500, and Arg531. Additionally, hydrophobic interactions with Ala478, Arg495, and Gln527, as well as a salt bridge with Glu146, enhance the stability of the binding.

The N-terminal part of SecA consists of three domains: the Nucleotide Binding Domain (NBD1), the Precursor Binding Domain (PDB), and the Intramolecular Regulator of ATPase 2 (IRA2, also known as NBD2). The spatial organization of NBD1 and IRA2 domains forms a clamp, and ATP hydrolysis occurs at the interface between these two domains. The NBD1 domain contains two high-affinity ATP binding sites, the highly conserved Walker A (aa residues 83-139) and Walker B (aa residues 205-227) motifs [30]. Interestingly, these four compounds have varying degrees of overlap with the NBD1 domain of SecA and all interact with Lys112. Alternatively, they could have allosteric effects on affecting NBD1 for ATPase activities. Overall, they can serve as potential inhibitors of S. aureus SecA1N75. Since there are extensive homologies of S. aureus SecA1N75 and S. aureus SecA2N75 (Fig. S1), these compounds could in fact have a dual target in affecting SecA1 and SecA2 domains.

3.3. Molecular Dynamics Simulation

In order to gain a deeper understanding of the conformational changes of protein ligand complexes under physiological conditions, 50 ns MD simulations were conducted on four complexes.

In our molecular dynamics simulations, we used the TIP3P water model, which is a standard three-point water model widely used in the simulation of biomolecules in solution. This model accounts for the interactions between water molecules and the protein, as well as other molecules, and is known for its fast simulation speed and high compatibility [53].

Root mean square deviation (RMSD) is used to measure the average change in the displacement of selected atoms in a given framework relative [54, 55]. In general, if the RMSD value of the ligand is smaller than that of the protein, it indicates that the ligand is tightly bound to the protein. For better comparison of the results, the RMSD curves of SW-569, SW-366, SW-849, and SW-2007 were plotted on the same coordinate system due to the similarity of their ligand structures (Fig. 3(a)).

SW-366 reaches 0.8 Å around 10 ns and stabilizes thereafter. SW-569 also reaches 0.8 Å around 10 ns and exhibits fluctuations within the range of 0.2 Å from 20-50 ns, indicating a relatively stable state. SW-849 reaches equilibrium within the range of 10-25 ns, with greater fluctuations within the range of 25-50 ns, and SW-569 shows a similar situation. SW-2007 exhibited the most noticeable fluctuation during the 50 ns simulation, which may be due to its greater flexibility. However, in the last 10 ns, SW-2007 fluctuated only between 1.0-1.25 Å, and this small range of fluctuation is considered to indicate equilibrium. This also explains why its binding energy is higher than that of the other three compounds. Interestingly, the three compounds, SW-366, SW-569, and SW-849, show very similar fluctuation trends. The data shows that the RMSD values of the protein backbone atoms of the ligands of these three compounds, SW-366, SW-569, and SW-849, except SW-2007, are close to each other and less than 1 Å, which suggests that the ligand binds with a great affinity. In conclusion, the hit ligands demonstrate stability during MD simulations, showing excellent consistency. Likewise, the radius of gyration (Rg) analysis reveals minimal fluctuations[56], suggesting a compact and stable system throughout the simulation, as illustrated in (Fig. 3(b)). To assess the flexibility and movement of residues during the simulation, we calculated the root mean square fluctuation (RMSF) values, shown in (Fig. 3(c)). With the exception of SW-366, most residues have RMSF values below 0.5 Å, indicating that secondary structure elements, such as α -helices and β -strands, are generally less flexible and more rigid compared to the ring regions.

The S. aureus SecA1N75-ligand complexes were analyzed to examine hydrogen bonding interactions. The results revealed that intermolecular hydrogen bonds were present in the SecA1N75-SW-366, SecA1N75-SW-569, SecA1N75-SW-849, and SecA1N75-SW-2007 complexes, confirming that these compounds effectively bind to SecA, forming stable protein-ligand complexes (Fig. 3(d)). Overall, the hydrogen bond analysis supports that the compounds form stable complexes with S. aureus SecA1N75.

The free energy landscape (FEL) [57] of protein tends to favor native folds. Using two principal components, RMSD and Rg, to generate the FEL of ligand-protein complexes helps in accurately understanding the minimal energy conformations of biomolecular assemblies. As shown in Fig. 4, the SecA-ligand complexes exhibit distinct minima in the FEL, indicating different stable conformations induced by ligand binding. The deep blue region in the figure corresponds to the low-energy or natural conformation, indicating the appearance of a highly stable conformation of the SecAligand system that emerged during the simulation.

To study the conformational changes of S. aureus SecA1N75 upon ligand binding, we performed a dynamics cross-correlation matrices (DCCM) analysis of Cα atoms to elucidate the interference between the fluctuations of correlated and anti-correlated atoms in the SecA system [58]. As

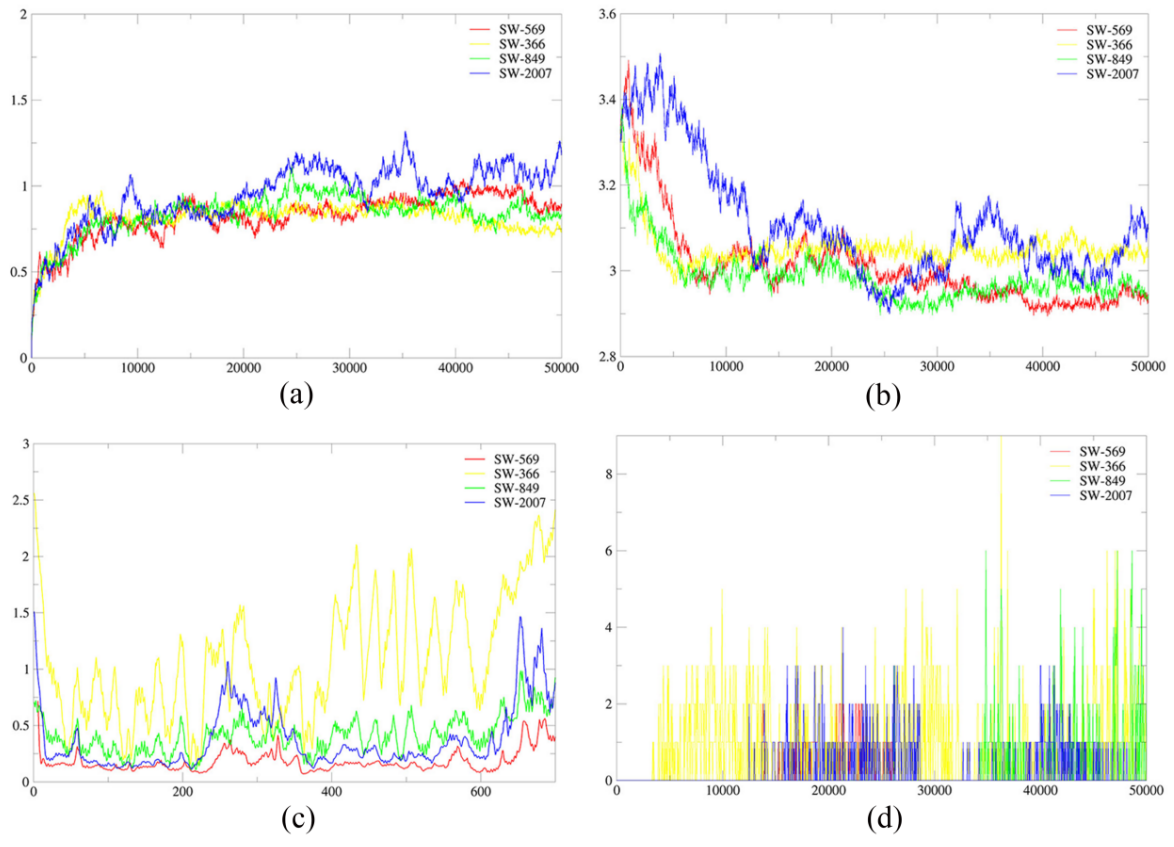


Fig. (3). MD simulation analysis. (a) RMSD of protein backbone; (b) Rg; (c) RMSF of protein backbone; (d) intermolecular hydrogen bonding. (A higher resolution / colour version of this figure is available in the electronic copy of the article).

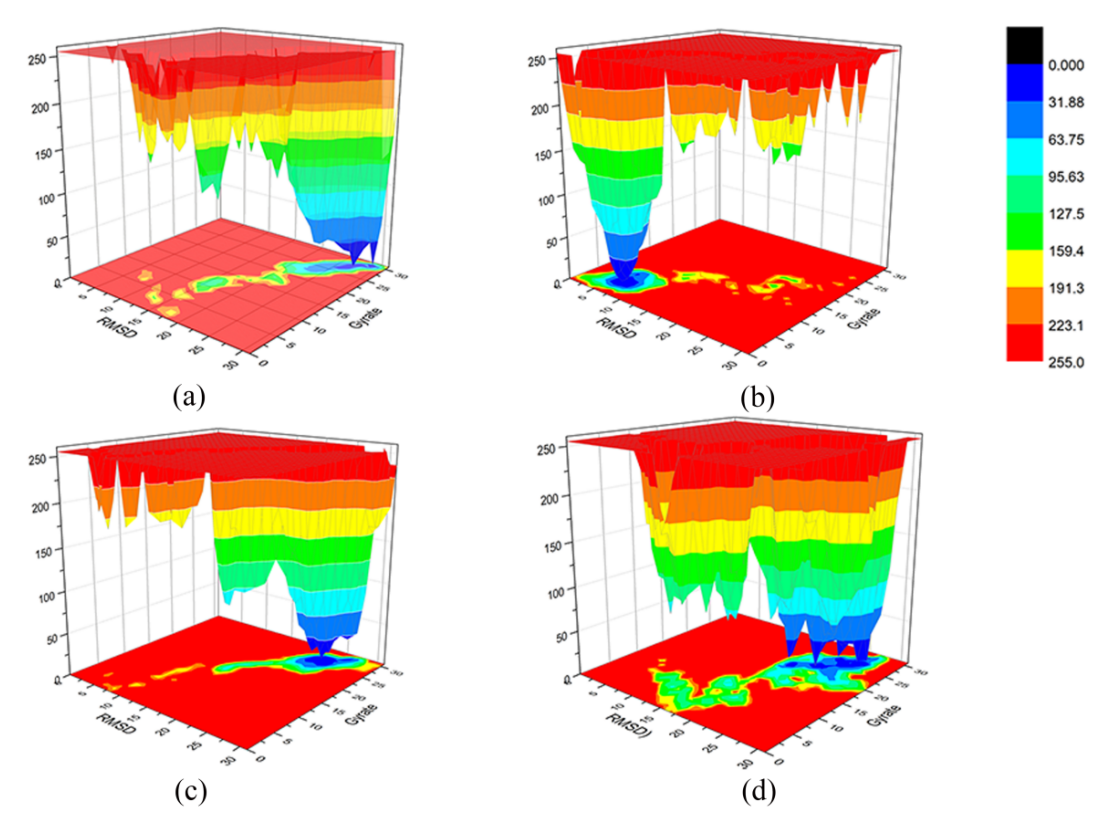


Fig. (4). Free energy landscapes of (a) SW-569, (b) SW-366, (c) SW-849, and (d) SW-2007. (A higher resolution / colour version of this figure is available in the electronic copy of the article).

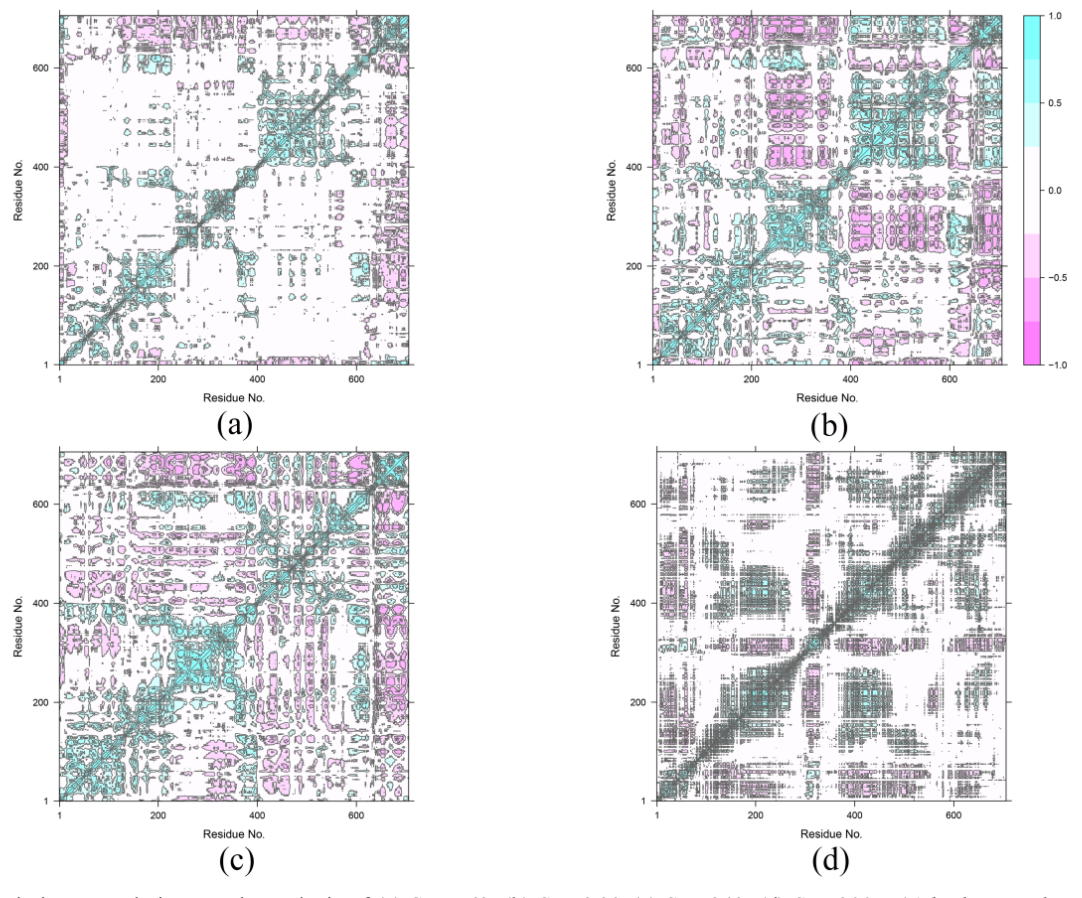


Fig. (5). Dynamic intercorrelation matrix analysis of (a) SW-569, (b) SW-366, (c) SW-849, (d) SW-2007, (A higher resolution / colour version of this figure is available in the electronic copy of the article).

shown in Fig. 5, the residuals can be seen along the diagonal line with the expected correlations. Some anti-correlation motions (pink regions) can be seen in the region away from the diagonal line, indicating that the fluctuating negative correlation between discontinuous residues in SecA is independent of motion. Notably, the two regions containing the SecA binding site exhibit strong correlated motions (cyan regions) in all systems, mainly represented by residues 1-200 and 420-590.

In addition, the degree of correlation/anti-correlation was relatively weaker for residues SW-569 and SW-2007 in that order. Overall structural changes in the protein were observed in the presence of the selected ligands, suggesting that these ligands can influence the conformation of S. aureus SecA1N75 protein.

3.4. Binding Free Energy Calculations

Extract the last 10 ns MD simulation trajectory for calculating binding free energy using the MM-PBSA method. The calculated binding free energies of SW-569, SW-366, SW-849, and SW-2007 were 1.500, -10.386, -18.227, and -21.076 kcal/mol, respectively. The lower the binding free energy, the higher the affinity between the receptor and the ligand. In other words, the normal function of the protein can be more effectively disrupted.

From the results, it is observed that the binding free energies of all the selected ligands except SW-569 are less than 13.642 kcal/mol, indicating strong binding energies and interactions between these ligands and S. aureus SecA1N75. Conversely, the binding free energy of SW-569 was greater than 0, suggesting that SW-569 could not bind spontaneously to the protein model. In summary, ligands other than SW-569 can serve as stable inhibitors of S. aureus SecA1N75 protein binding.

In addition, we can analyze the contribution of each amino acid one by one and label the top five amino acids with the highest contribution (Fig. S3), which is not entirely consistent with the ATP binding sites displayed on UniProt (https://www.uniprot.org/). This means that these candidate compounds may not compete with ATP and may affect ATP binding sites allosterically.

3.5. ADME-T Properties

Next, studying the physicochemical properties, pharmacokinetics, and potential toxicity of candidate compounds is an essential step as potential inhibitors. The pharmacokinetic parameters (ADME-T) [59] are shown in Table 2. Lipinski's rule is an empirical rule in the field of drug discovery used to evaluate whether a compound has good drug properties. According to the data, it can be seen that SW-2007 does not comply with Lipinski's rule, but this does not negate the possibility of SW-2007 as a potential drug [60]. The TPSA values of the hit compounds are all less than 145 Å2, indicating their potential to be developed into oral medication. In addition, only SW-569 and SW-2007 had high GI values, indicating widely absorbed in the intestine. None of the four compounds could cross the blood-brain barrier. Based on toxicity predictions, only SW-849 has very low carcinogenic potential and is neither mutagenic nor nephrotoxic. Therefore, this compound is less hazardous. In conclusion, SW-849 shows promising pharmacological effects and can be further developed as anti-S. aureus drugs.

ADME-T properties are essential for evaluating a compound's pharmacokinetics. Molecular weight (MW) affects absorption and distribution, while cLogP indicates lipophilicity and membrane permeability. Rotatable bonds (rBonds) influence molecular flexibility. Hydrogen-bond acceptors (HBA) and donors (HBD) determine interactions with biomolecules, and topological polar surface area (TPSA) reflects polarity. Gastrointestinal absorption (GI) measures drug uptake in the gut, and blood-brain barrier permeability (BBB) indicates the compound's ability to cross the blood-brain barrier. These properties help predict a compound's drug-likeness and bioavailability.

3.6. Virtual Screened SecA Inhibitors: Old Drugs and New Target?

These 4 compounds as *S. aureus* SecA1N75 inhibitors, were identified via virtual screening [60, 61] turn out to be related to some known drugs for various treatments, raising the question of whether these might be the old drugs with new targets.

Compound SW-569 turns out to be related to Conivaptan, which is a dual vasopressin V1a and V2 receptor antagonist [62-64]. By blocking the action of vasopressin at these receptors, it leads to increased renal water excretion, thereby treating hyponatremia caused by conditions such as the Syndrome of Inappropriate Antidiuretic Hormone Secretion

(SIADH). Conivaptan has also been studied for use in patients with acute decompensated heart failure, where fluid overload can exacerbate symptoms. By promoting water excretion, it helps reduce fluid retention and may improve symptoms associated with heart failure [63].

Compound SW-366 is related to Regorafenib, which is an oral multi-targeted tyrosine kinase inhibitor used for the treatment of various types of cancer [65, 66]. It primarily acts by inhibiting multiple angiogenic factors (such as VEGF receptors) [67], tumor cell growth factors (such as FGFR, PDGFR) [68, 69], and other related signaling pathways. Regorafenib has also demonstrated efficacy in patients with advanced GIST who are either unresectable or resistant to Imatinib treatment [70].

Compound SW-849 is related to Glipizide, which is an oral sulfonylurea drug primarily used to treat type 2 diabetes. It helps control blood glucose levels by increasing insulin secretion from the pancreas [71, 72]. Glipizide can also be used in combination with other antidiabetic medications, such as Metformin and Thiazolidinediones, to enhance blood glucose control [73]. Furthermore, compared to other sulfonylureas, Glipizide has a shorter half-life, which helps reduce the risk of hypoglycemia and allows for a more flexible dosing regimen.

Compound SW-2007 is related to Abemaciclib, which is an oral selective CDK4/6 inhibitor [74]. It prevents cancer cell proliferation by inhibiting cyclin-dependent kinases 4 and 6 (CDK4/6) and is primarily used in the treatment of breast cancer [75], especially for advanced estrogen receptor-positive (ER+) and HER2-negative breast cancer [76].

For the drug targets clearly understood above, SW-569 acts on the kidneys and blood vessels, SW-366 and SW-2007 target cancer cells, and SW-849 acts on the pancreas. Since SecA is not present in mammals, there is no direct relationship between the targets of these known drugs and SecA. However, there are currently no clinical cases involving the simultaneous treatment of drug-resistant bacteria with can-

Table 2 Physical and chemic	al properties and toxicity predictions.
1 abic 2. I mysical and chemic	ai properties and toxicity predictions.

Pharmacokinetics	SW-569	SW-366	SW-849	SW-2007
MW (≤500 Da)	498.57	482.82	445.54	506.59
cLogP (≤5)	5.01	4.41	1.97	4.04
rBonds (≤10)	6	9	10	7
HBA (≤10)	3	8	6	8
HBD (≤5)	2	3	3	1
Lipinski	0	0	0	1
TPSA (Å2) (≤145)	78.09	92.35	138.53	75
GI	High	Low	Low	High
BBB	No	No	No	No
Carcinogenicity	0.616	0.313	0.034	0.823
Mutagenesis	1	1	0	1

cer, diabetes, or diuretics. We believe that, in the field of "drug repurposing," these compounds are worth further investigation.

The four potential SecA inhibitors identified here have established clinical uses for other treatments. These compounds need to be further evaluated as SecA inhibitors. So far, the best-known SecA inhibitors are in the range of submicromolars [15]. By re-evaluating the potential of these traditional drugs and comparing the effective doses esp with AutoDock inhibition constants, at nM, two with inhibition constants at 10-5 to 10-7 nM as shown in Table 1. Though these compounds were found by screening non-ATP binding domains, work in progress indicates that they affect ATPase activities, in addition to antimicrobial activities. If there are more effective than the known SecA inhibitors, they could be interesting new lead compounds to develop. Previous reports indicated that SecA inhibitors are not subject to the levels of efflux pumps [15, 29]. We will further explore their applications in treating multiple-drug-resistant strains and new diseases or symptoms. This process not only reveals their new value in modern medicine but also provides fresh perspectives and possibilities for drug repurposing for new targets.

CONCLUSION

In this study, structure-based virtual screening was conducted to identify novel inhibitors targeting the non-ATP binding domain of S. aureus SecA1N75. First, a crystal model of S. aureus SecA1N75 was successfully built through homology modeling. The homology modeling, molecular docking, and molecular dynamics simulation results indicated high stability and strong binding free energies in this complex system. In conclusion, this study demonstrates the optimal binding characteristics of four lead compounds and lays a foundation for the further development of antibacterial drugs targeting the non-ATP binding domain of S. aureus simulations. These compounds have been clinically used, but SecA could be another new-found target for treating bacterial infection. In subsequent research on S. aureus, three compounds (SW-366, SW-849, and SW-2007) could be proposed as potential candidate drugs against S. aureus. We will explore their enzyme inhibition, anti-S. aureus and other bacterial activities, secretion of virulence factors, and their impact on bypassing efflux pumps.

AUTHORS' CONTRIBUTIONS

It is hereby acknowledged that all authors have accepted responsibility for the manuscript's content and consented to its submission. They have meticulously reviewed all results and unanimously approved the final version of the manuscript.

ETHICS APPROVAL AND CONSENT TO PARTICI-**PATE**

Not applicable.

HUMAN AND ANIMAL RIGHTS

Not applicable.

CONSENT FOR PUBLICATION

Not applicable.

AVAILABILITY OF DATA AND MATERIALS

The data and supportive information are available within the article.

FUNDING

This work was supported in parts by the Natural Science Foundation of Sichuan Province (No. 23NSFSC0920).

CONFLICT OF INTEREST

The authors declare no conflict of interest, financial or otherwise.

ACKNOWLEDGEMENTS

We would like to thank the Analysis and Testing Center of Southwest Jiaotong University for providing help in equipment and analysis.

REFERENCES

- Liu, C.; Bayer, A.; Cosgrove, S.E.; Daum, R.S.; Fridkin, S.K.; Gorwitz, R.J.; Kaplan, S.L.; Karchmer, A.W.; Levine, D.P.; Murray, B.E.; J Rybak, M.; Talan, D.A.; Chambers, H.F. Clinical practice guidelines by the infectious diseases society of america for the treatment of methicillin-resistant Staphylococcus aureus infections in adults and children: Executive summary. Clin. Infect. Dis., 2011, 52(3), 285-292. http://dx.doi.org/10.1093/cid/cir034 PMID: 21217178
- [2] Grispoldi, L.; Karama, M.; Armani, A.; Hadjicharalambous, C.; Cenci-Goga, B.T. Staphylococcus aureus enterotoxin in food of animal origin and staphylococcal food poisoning risk assessment from farm to table. Ital J. Anim. Sci., 2021, 20(1), 677-690. http://dx.doi.org/10.1080/1828051X.2020.1871428
- [3] Permyakov, E.A.; Regenthal, P.; Hansen, J.S.; André, I.; Lindkvist-Petersson, K. Thermal stability and structural changes in bacterial toxins responsible for food poisoning. PLoS One, 2017, ..., 12.
- Ramadan, H.A.; El-Baz, A.M.; Goda, R.M.; El-Sokkary, M.M.A.; [4] El-Morsi, R.M. Molecular characterization of enterotoxin genes in methicillin-resistant S. aureus isolated from food poisoning outbreaks in Egypt. J. Health. Popul. Nutr., 2023, 42(1), 86. http://dx.doi.org/10.1186/s41043-023-00416-z PMID: 37641155
- Turner, N.A.; Sharma-Kuinkel, B.K.; Maskarinec, S.A.; Eichen-[5] berger, E.M.; Shah, P.P.; Carugati, M.; Holland, T.L.; Fowler, V.G. Methicillin-resistant Staphylococcus aureus: An overview of basic and clinical research. Nat. Rev. Microbiol., 2019, 17(4), 203-218. http://dx.doi.org/10.1038/s41579-018-0147-4 PMID: 30737488
- [6] Ippolito, G.; Leone, S.; Lauria, F.N.; Nicastri, E.; Wenzel, R.P. Methicillin-resistant Staphylococcus aureus: The superbug. Int. J. Infect. Dis., 2010, 14, S7-S11.(Suppl. 4) http://dx.doi.org/10.1016/j.ijid.2010.05.003 PMID: 20851011
- Hu, J.; Akula, N.; Wang, N. Development of a microemulsion formulation for antimicrobial SecA inhibitors. PLoS One, 2016, 11(3), e0150433.
 - http://dx.doi.org/10.1371/journal.pone.0150433 PMID: 26963811
- Kavanagh, K.T. Control of MSSA and MRSA in the United States: [8] Protocols, policies, risk adjustment and excuses. Antimicrob Resist Infect. Control., 2019, 8(1), 103.
- http://dx.doi.org/10.1186/s13756-019-0550-2 PMID: 31244994 [9] Zhang, Z.; Han, Q.; Mao, X.; Liu, J.; Wang, W.; Li, D.; Zhou, F.; Ke, Y.; Xu, L.; Hu, L. Discovery of novel SecA inhibitors against ' Candidatus Liberibacter asiaticus" through virtual screening and biological evaluation. Chem. Biol. Drug Des, 2021, 98(3), 395-404. http://dx.doi.org/10.1111/cbdd.13859 PMID: 33963664

- [10] Jian, T.; Su, Q.; Liu, Y.; Seoh, H.K.; Houghton, J.E.; Tai, P.C.; Huang, X. Structure-based virtual screening of *Helicobacter pylori* SecA inhibitors. *IEEE Trans Nanobiosci*, 2023, 22(4), 933-942. http://dx.doi.org/10.1109/TNB.2023.3259946 PMID: 37030876
- [11] Cranford-Smith, T.; Huber, D. The way is the goal: How SecA transports proteins across the cytoplasmic membrane in bacteria. FEMS Microbiol. Lett, 2018, 365(11), 365. http://dx.doi.org/10.1093/femsle/fny093 PMID: 29790985
- [12] Feltcher, M.E.; Braunstein, M. Emerging themes in SecA2-mediated protein export. Nat. Rev. Microbiol., 2012, 10(11), 779-789. http://dx.doi.org/10.1038/nrmicro2874 PMID: 23000954
- [13] Tsirigotaki, A.; De Geyter, J.; Šoštaric', N.; Economou, A.; Karamanou, S. Protein export through the bacterial Sec pathway. *Nat. Rev. Microbiol.*, 2017, 15(1), 21-36. http://dx.doi.org/10.1038/nrmicro.2016.161 PMID: 27890920
- [14] Gupta, R.; Toptygin, D.; Kaiser, C.M. The SecA motor generates mechanical force during protein translocation. *Nat. Commun*, 2020, 11(1), 3802. http://dx.doi.org/10.1038/s41467-020-17561-2 PMID: 32732903
- [15] Jin, J.; Hsieh, Y.H.; Chaudhary, A.S.; Cui, J.; Houghton, J.E.; Sui, S.; Wang, B.; Tai, P.C. SecA inhibitors as potential antimicrobial agents: Differential actions on SecA-only and SecA-SecYEG protein-conducting channels. FEMS Microbiol. Lett, 2018, 365(15), fny145.
- http://dx.doi.org/10.1093/femsle/fny145 PMID: 30007321
 [16] Hu, H.J.; Holley, J.; He, J.; Harrison, R.W.; Yang, H.; Tai, P.C.; Pan, Y. To be or not to be: Predicting soluble SecAs as membrane proteins. *IEEE Trans Nanobiosci*, **2007**, *6*(2), 168-179. http://dx.doi.org/10.1109/TNB.2007.897486 PMID: 17695753
- [17] Zulauf, K.E.; Sullivan, J.T.; Braunstein, M.; Braunstein, M. The SecA2 pathway of Mycobacterium tuberculosis exports effectors that work in concert to arrest phagosome and autophagosome maturation. *PLoS Pathog*, 2018, 14(4), e1007011. http://dx.doi.org/10.1371/journal.ppat.1007011 PMID: 29709019
- [18] Prabudiansyah, I.; Kusters, I.; Driessen, A.J.M.; Driessen, A.J.M. In vitro interaction of the housekeeping SecA1 with the accessory SecA2 protein of mycobacterium tuberculosis. PLoS One, 2015, 10(6), e0128788. http://dx.doi.org/10.1371/journal.pone.0128788 PMID: 26047312
- [19] Ligon, L.S.; Rigel, N.W.; Romanchuk, A.; Jones, C.D.; Braunstein, M. Suppressor analysis reveals a role for SecY in the SecA2-dependent protein export pathway of Mycobacteria. *J. Bacteriol.*, 2013, 195(19), 4456-4465. http://dx.doi.org/10.1128/JB.00630-13 PMID: 23913320
- [20] Li, M.; Huang, Y.J.; Tai, P.C.; Wang, B. Discovery of the first SecA inhibitors using structure-based virtual screening. *Biochem. Biophys. Res. Commun*, 2008, 368(4), 839-845. http://dx.doi.org/10.1016/j.bbrc.2008.01.135 PMID: 18261984
- [21] Akula, N.; Zheng, H.; Han, F.Q.; Wang, N. Discovery of novel SecA inhibitors of Candidatus Liberibacter asiaticus by structure based design. *Bioorg Med. Chem. Lett*, 2011, 21(14), 4183-4188. http://dx.doi.org/10.1016/j.bmcl.2011.05.086 PMID: 21684161
- [22] Sugie, Y.; Inagaki, S.; Kato, Y.; Nishida, H.; Pang, C.H.; Saito, T.; Sakemi, S.; Dib-Hajj, F.; Mueller, J.P.; Sutcliffe, J.; Kojima, Y. CJ-21,058, a new SecA inhibitor isolated from a fungus. *J. Antibiot.*, 2002, 55(1), 25-29. http://dx.doi.org/10.7164/antibiotics.55.25 PMID: 11918061
- [23] Oliver, D.B.; Cabelli, R.J.; Dolan, K.M.; Jarosik, G.P. Azide-resistant mutants of Escherichia coli alter the SecA protein, an azide-sensitive component of the protein export machinery. *Proc Natl Acad. Sci. USA*, 1990, 87(21), 8227-8231. http://dx.doi.org/10.1073/pnas.87.21.8227 PMID: 2146683
- [24] Yu, W.; Li-Li, Z.; Qiu-Ping, L.; Qiu-Ping, L. The establishment and application of inhibitors screening model targeting to Pseudomonas aeruginosa SecA ATPase. *Microbiology*, 2013, 2037(2012), 1771-1778
- [25] Cui, J.; Jin, J.; Hsieh, Y.H.; Yang, H.; Ke, B.; Damera, K.; Tai, P.C.; Wang, B. Design, synthesis and biological evaluation of rose bengal analogues as SecA inhibitors. *ChemMedChem*, 2013, 8(8), 1384-1393. http://dx.doi.org/10.1002/cmdc.201300216 PMID: 23794293
- [26] Huang, Y.J.; Wang, H.; Gao, F.B.; Li, M.; Yang, H.; Wang, B.; Tai, P.C. Fluorescein analogues inhibit SecA ATPase: The first

- sub-micromolar inhibitor of bacterial protein translocation. *ChemMedChem,* **2012**, 7(4), 571-577. http://dx.doi.org/10.1002/cmdc.201100594 PMID: 22354575
- [27] Chaudhary, A.S.; Jin, J.; Chen, W.; Tai, P.C.; Wang, B. Design, syntheses and evaluation of 4-oxo-5-cyano thiouracils as SecA inhibitors. *Bioorg Med. Chem.*, 2015, 23(1), 105-117. http://dx.doi.org/10.1016/j.bmc.2014.11.017 PMID: 25498235
- [28] Jin, J.; Hsieh, Y.H.; Cui, J.; Damera, K.; Dai, C.; Chaudhary, A.S.; Zhang, H.; Yang, H.; Cao, N.; Jiang, C.; Vaara, M.; Wang, B.; Tai, P.C. Using chemical probes to assess the feasibility of targeting SecA for developing antimicrobial agents against gram-negative bacteria. *ChemMedChem*, 2016, 11(22), 2511-2521. http://dx.doi.org/10.1002/cmdc.201600421 PMID: 27753464
- [29] Jin, J.; Cui, J.; Chaudhary, A.S.; Hsieh, Y.H.; Damera, K.; Zhang, H.; Yang, H.; Wang, B.; Tai, P.C. Evaluation of small molecule SecA inhibitors against methicillin-resistant Staphylococcus aure-us. *Bioorg Med. Chem.*, 2015, 23(21), 7061-7068. http://dx.doi.org/10.1016/j.bmc.2015.09.027 PMID: 26432604
- [30] Ambroziak, P.; Rzepka, I.; Skorko-Glonek, J. SecA A multidomain and multitask bacterial export protein. *Acta. Biochim Pol*, 2021, 68(3), 427-436. http://dx.doi.org/10.18388/abp.2020 5761 PMID: 34463460
- [31] Ghai, I. Electrophysiological insights into antibiotic translocation and resistance: The impact of outer membrane proteins. *Membranes*, **2024**, *14*(7), 161.
- http://dx.doi.org/10.3390/membranes14070161 PMID: 39057669

 [32] De Waelheyns, E.; Segers, K.; Sardis, M.F.; Anné, J.; Nicolaes, G.A.F.; Economou, A. Identification of small-molecule inhibitors against SecA by structure-based virtual ligand screening. *J. Antibiot.*, 2015, 68(11), 666-673. http://dx.doi.org/10.1038/ja.2015.53 PMID: 25990955
- [33] Cerovsky, C.; Jin, J.; Yang, H.; Wang, B.; Tai, P.C. Evaluation of the seca inhibitors as novel anti-microbial agents. DISCOVERY Georgia State Hons Coll Undergrad Res. J., 2012, 1(12) http://dx.doi.org/10.31922/disc1.12
- [34] Chaudhary, A.S.; Chen, W.; Jin, J.; Tai, P.C.; Wang, B.; Sec, A. SecA: A potential antimicrobial target. *Future Med. Chem.*, 2015, 7(8), 989-1007.
 http://dx.doi.org/10.4155/fmc.15.42 PMID: 26062397
- [35] Jamshad, M.; Knowles, T.J.; White, S.A.; Ward, D.G.; Mohammed, F.; Rahman, K.F.; Wynne, M.; Hughes, G.W.; Kramer, G.; Bukau, B.; Huber, D. The C-terminal tail of the bacterial translocation ATPase SecA modulates its activity. *eLife*, **2019**, 8, e48385. http://dx.doi.org/10.7554/eLife.48385 PMID: 31246174
- [36] Melly, G.C.; Stokas, H.; Davidson, P.M.; Roma, J.S.; Rhodes, H.L.; Purdy, G.E. Identification of residues important for *M. tuber-culosis* MmpL11 function reveals that function is modulated by phosphorylation in the C-terminal domain. *Mol. Microbiol.*, 2021, 115(2), 208-221.
- http://dx.doi.org/10.1111/mmi.14611 PMID: 32985735
- [37] Biasini, M.; Bienert, S.; Waterhouse, A.; Arnold, K.; Studer, G.; Schmidt, T.; Kiefer, F.; Cassarino, T.G.; Bertoni, M.; Bordoli, L.; Schwede, T. SWISS-MODEL: Modelling protein tertiary and quaternary structure using evolutionary information. *Nucleic Acids Res.*, 2014, 42(W1), W252-W258. http://dx.doi.org/10.1093/nar/gku340 PMID: 24782522
- [38] Colovos, C.; Yeates, T.O. Verification of protein structures: Patterns of nonbonded atomic interactions. *Protein Sci.*, 1993, 2(9), 1511-1519. http://dx.doi.org/10.1002/pro.5560020916 PMID: 8401235
- [39] Lüthy, R.; Bowie, J.U.; Eisenberg, D. Assessment of protein models with three-dimensional profiles. *Nature*, **1992**, *356*(6364), 83-85. http://dx.doi.org/10.1038/356083a0 PMID: 1538787
- [40] Laskowski, R.A.; MacArthur, M.W.; Moss, D.S.; Thornton, J.M. PROCHECK: A program to check the stereochemical quality of protein structures. J. Appl. Cryst. 1993, 26(2), 283-291. http://dx.doi.org/10.1107/S0021889892009944
- [41] Trott, O.; Olson, A.J. AutoDock Vina: Improving the speed and accuracy of docking with a new scoring function, efficient optimization, and multithreading. *J. Comput. Chem.*, **2010**, *31*(2), 455-461.
 - http://dx.doi.org/10.1002/jcc.21334 PMID: 19499576

- [42] Adasme, M.F.; Linnemann, K.L.; Bolz, S.N.; Kaiser, F.; Salentin, S.; Haupt, V.J.; Schroeder, M. PLIP 2021: Expanding the scope of the protein-ligand interaction profiler to DNA and RNA. Nucleic Acids Res., 2021, 49(W1), W530-W534. http://dx.doi.org/10.1093/nar/gkab294 PMID: 33950214
- [43] Kagami, L.; Wilter, A.; Diaz, A.; Vranken, W. The ACPYPE web server for small-molecule MD topology generation. Bioinformatics, 2023, 39(6), btad350. http://dx.doi.org/10.1093/bioinformatics/btad350 PMID: 37252824
- Duan, Y.; Wu, C.; Chowdhury, S.; Lee, M.C.; Xiong, G.; Zhang, [44] W.; Yang, R.; Cieplak, P.; Luo, R.; Lee, T.; Caldwell, J.; Wang, J.; Kollman, P. A point-charge force field for molecular mechanics simulations of proteins based on condensed-phase quantum mechanical calculations. J. Comput. Chem., 2003, 24(16), 1999-2012. http://dx.doi.org/10.1002/jcc.10349 PMID: 14531054
- [45] Van Der Spoel, D.; Lindahl, E.; Hess, B.; Groenhof, G.; Mark, A.E.; Berendsen, H.J.C. GROMACS: Fast, flexible, and free. J. Comput. Chem., 2005, 26(16), 1701-1718. http://dx.doi.org/10.1002/icc.20291 PMID: 16211538
- [46] Genheden, S.; Ryde, U. The MM/PBSA and MM/GBSA methods to estimate ligand-binding affinities. Expert Opin. Drug Discov, 2015, 10(5), 449-461. http://dx.doi.org/10.1517/17460441.2015.1032936 PMID: 25835573
- [47] Homeyer, N.; Gohlke, H. Free energy calculations by the molecular mechanics poisson-boltzmann surface area method. Mol. Inform., **2012**, 31(2), 114-122. http://dx.doi.org/10.1002/minf.201100135 PMID: 27476956
- Ding, H.; Yin, Y.; Ni, S.; Sheng, Y.; Ma, Y. Accurate evaluation on [48] the interactions of SARS-CoV-2 with its receptor ACE2 and antibodies CR3022/CB6*. Chin Phys. Lett, 2021, 38(1), 018701. http://dx.doi.org/10.1088/0256-307X/38/1/018701
- [49] Daina, A.; Michielin, O.; Zoete, V. SwissADME: A free web tool to evaluate pharmacokinetics, drug-likeness and medicinal chemistry friendliness of small molecules. Sci. Rep, 2017, 7(1), 42717. http://dx.doi.org/10.1038/srep42717 PMID: 28256516
- [50] Yang, H.; Lou, C.; Sun, L.; Li, J.; Cai, Y.; Wang, Z.; Li, W.; Liu, G.; Tang, Y. admetSAR 2.0: Web-service for prediction and optimization of chemical ADMET properties. Bioinformatics, 2019, 35(6), 1067-1069. http://dx.doi.org/10.1093/bioinformatics/bty707 PMID: 30165565
- [51] Studer, G.; Rempfer, C.; Waterhouse, A.M.; Gumienny, R.; Haas, J.; Schwede, T. QMEANDisCo-distance constraints applied on model quality estimation. Bioinformatics, 2020, 36(8), 2647. http://dx.doi.org/10.1093/bioinformatics/btaa058 PMID: 32048708
- [52] Robert, X.; Gouet, P. Deciphering key features in protein structures with the new ENDscript server. Nucleic Acids Res., 2014, 42(W1), W320-W324. http://dx.doi.org/10.1093/nar/gku316 PMID: 24753421
- Sethi, A.; Agrawal, N.; Brezovsky, J. Impact of water models on [53] the structure and dynamics of enzyme tunnels. Comput. Struct. Biotechnol. J., 2024, 23, 3946-3954. http://dx.doi.org/10.1016/j.csbj.2024.10.051 PMID: 39582894
- [54] Aier, I.; Varadwaj, P.K.; Raj, U. Structural insights into conformational stability of both wild-type and mutant EZH2 receptor. Sci. Rep, 2016, 6(1), 34984. http://dx.doi.org/10.1038/srep34984 PMID: 27713574
- [55] Lu, S.Y.; Jiang, Y.J.; Lv, J.; Wu, T.X.; Yu, Q.S.; Zhu, W.L. Molecular docking and molecular dynamics simulation studies of GPR40 receptor-agonist interactions. J. Mol. Graph Model, 2010, 28(8), 766-774. http://dx.doi.org/10.1016/j.jmgm.2010.02.001 PMID: 20227312
- [56] Xiang, C.; Chen, C.; Li, X.; Wu, Y.; Xu, Q.; Wen, L.; Xiong, W.; Liu, Y.; Zhang, T.; Dou, C.; Ding, X.; Hu, L.; Chen, F.; Yan, Z.; Liang, L.; Wei, G. Computational approach to decode the mechanism of curcuminoids against neuropathic pain. Comput. Biol. Med., 2022, 147, 105739. http://dx.doi.org/10.1016/j.compbiomed.2022.105739 PMID:
- [57] Tavernelli, I.; Cotesta, S.; Di Iorio, E.E. Protein dynamics, thermal stability, and free-energy landscapes: A molecular dynamics investigation. Biophys. J., 2003, 85(4), 2641-2649. http://dx.doi.org/10.1016/S0006-3495(03)74687-6 PMID: 14507727

- [58] Jha, R.K.; Jabeer Khan, R.; Singh, E.; Kumar, A.; Jain, M.; Muthukumaran, J.; Singh, A.K. An extensive computational study to identify potential inhibitors of Acyl-homoserine-lactone synthase from Acinetobacter baumannii (strain AYE). J. Mol. Graph Model, **2022**, 114, 108168.
- http://dx.doi.org/10.1016/j.jmgm.2022.108168 PMID: 35339024 [59] Lucas, A.J.; Sproston, J.L.; Barton, P.; Riley, R.J. Estimating human ADME properties, pharmacokinetic parameters and likely clinical dose in drug discovery. Expert Opin. Drug Discov, 2019, 14(12), 1313-1327. http://dx.doi.org/10.1080/17460441.2019.1660642 PMID: 31538500
- [60] Lipinski, C.A. Lead- and drug-like compounds: The rule-of-five revolution. Drug Discov Today Technol, 2004, 1(4), 337-341. http://dx.doi.org/10.1016/j.ddtec.2004.11.007 PMID: 24981612
- [61] Wilton, D.; Willett, P.; Lawson, K.; Mullier, G. Comparison of ranking methods for virtual screening in lead-discovery programs. J. Chem. Inf Comput. Sci., 2003, 43(2), 469-474. http://dx.doi.org/10.1021/ci025586i PMID: 12653510
- Marbury, T.; Fox, J.; Kaelin, B.; Pavliv, L. Pharmacokinetics of [62] conivaptan use in patients with severe hepatic impairment. Drug Des Devel Ther., 2017, 11, 373-382. http://dx.doi.org/10.2147/DDDT.S125459 PMID: 28243060
- Goldsmith, S.R.; Udelson, J.E.; Gheorghiade, M. Dual vasopressin [63] V1a/V2 antagonism: The next step in neurohormonal modulation in patients with heart failure? J. Card Fail, 2018, 24(2), 112-114 http://dx.doi.org/10.1016/j.cardfail.2017.12.011 PMID: 29329950
- [64] Manning, M.; Stoev, S.; Chini, B.; Durroux, T.; Mouillac, B.; Guillon, G. Peptide and non-peptide agonists and antagonists for the vasopressin and oxytocin V1a, V1b, V2 and OT receptors: Research tools and potential therapeutic agents ★. Prog Brain Res., 2008, 170, 473-512. http://dx.doi.org/10.1016/S0079-6123(08)00437-8 PMID: 18655903
- [65] Van Cutsem, E.; Martinelli, E.; Cascinu, S.; Sobrero, A.; Banzi, M.; Seitz, J.F.; Barone, C.; Ychou, M.; Peeters, M.; Brenner, B.; Hofheinz, R.D.; Maiello, E.; André, T.; Spallanzani, A.; Garcia-Carbonero, R.; Arriaga, Y.E.; Verma, U.; Grothey, A.; Kappeler, C.; Miriyala, A.; Kalmus, J.; Falcone, A.; Zaniboni, A. Regorafenib for patients with metastatic colorectal cancer who progressed after standard therapy: Results of the large, single-arm, open-label phase IIIb CONSIGN study. Oncologist, 2019, 24(2), 185-192. http://dx.doi.org/10.1634/theoncologist.2018-0072 PMID:
- Demetri, G.D.; Reichardt, P.; Kang, Y.K.; Blay, J.Y.; Rutkowski, [66] P.; Gelderblom, H.; Hohenberger, P.; Leahy, M.; von Mehren, M.; Joensuu, H.; Badalamenti, G.; Blackstein, M.; Le Cesne, A.; Schöffski, P.; Maki, R.G.; Bauer, S.; Nguyen, B.B.; Xu, J.; Nishida, T.; Chung, J.; Kappeler, C.; Kuss, I.; Laurent, D.; Casali, P.G. Efficacy and safety of regorafenib for advanced gastrointestinal stromal tumours after failure of imatinib and sunitinib (GRID): An international, multicentre, randomised, placebo-controlled, phase 3 trial. Lancet. 2013. 381(9863), 295-302. http://dx.doi.org/10.1016/S0140-6736(12)61857-1 PMID:
- [67] Rimassa, L.; Pressiani, T.; Personeni, N.; Santoro, A. Regorafenib for the treatment of unresectable hepatocellular carcinoma. Expert Rev. Anticancer Ther., 2017, 17(7), 567-576. http://dx.doi.org/10.1080/14737140.2017.1338955 PMID: 28580808
- [68] Lau, D.K.; Luk, I.Y.; Jenkins, L.J.; Martin, A.; Williams, D.S.; Schoffer, K.L.; Chionh, F.; Buchert, M.; Sjoquist, K.; Boussioutas, A.; Hayes, S.A.; Ernst, M.; Weickhardt, A.J.; Pavlakis, N.; Tebbutt, N.C.; Mariadason, J.M. Rapid resistance of FGFR-driven gastric cancers to regorafenib and targeted FGFR inhibitors can be overcome by parallel inhibition of MEK. Mol. Cancer Ther., 2021, 20(4), 704-715. http://dx.doi.org/10.1158/1535-7163.MCT-20-0836 PMID:
- [69] Mongiardi, M.P.; Pallini, R.; D'Alessandris, Q.G.; Levi, A.; Falchetti, M.L. Regorafenib and glioblastoma: A literature review of preclinical studies, molecular mechanisms and clinical effectiveness. Expert Rev. Mol. Med., 2024, 26, e5. http://dx.doi.org/10.1017/erm.2024.8 PMID: 38563164

- [70] Grothey, A.; Cutsem, E.V.; Sobrero, A.; Siena, S.; Falcone, A.; Ychou, M.; Humblet, Y.; Bouché, O.; Mineur, L.; Barone, C.; Adenis, A.; Tabernero, J.; Yoshino, T.; Lenz, H.J.; Goldberg, R.M.; Sargent, D.J.; Cihon, F.; Cupit, L.; Wagner, A.; Laurent, D.; Group, C.S. Regorafenib monotherapy for previously treated metastatic colorectal cancer (CORRECT): An international, multicentre, randomised, placebo-controlled, phase 3 trial. *Lancet*, 2013, 381(9863), 303-312. http://dx.doi.org/10.1016/S0140-6736(12)61900-X PMID: 23177514
- [71] Aroda, V.R.; Edelstein, S.L.; Goldberg, R.B.; Knowler, W.C.; Marcovina, S.M.; Orchard, T.J.; Bray, G.A.; Schade, D.S.; Temprosa, M.G.; White, N.H.; Crandall, J.P. Long-term metformin use and vitamin b12 deficiency in the diabetes prevention program outcomes study. J. Clin. Endocrinol. Metab., 2016, 101(4), 1754-1761.
- http://dx.doi.org/10.1210/jc.2015-3754 PMID: 26900641
 [72] Ford, S.L. NIDDM in the cat: Treatment with the oral hypoglycemic medication, glipizide. *Vet. Clin. North Am Small Anim. Pract,* 1995, 25(3), 599-615.
 http://dx.doi.org/10.1016/S0195-5616(95)50056-7 PMID: 7660535
- [73] Shaikh, S.; Vaidya, V.; Gupta, A.; Kulkarni, R.; Joshi, A.; Kulkarni, M.; Sharma, V.; Revankar, S. A review on affordable combinations in type 2 diabetes care: Exploring the cost-effective potential of glipizide + metformin and glimepiride + metformin + pioglitazone. *Cureus*, 2024, 16(5), e59850.

- http://dx.doi.org/10.7759/cureus.59850 PMID: 38854289
- [74] Braal, C.L.; Jongbloed, E.M.; Wilting, S.M.; Mathijssen, R.H.J.; Koolen, S.L.W.; Jager, A. Inhibiting CDK4/6 in breast cancer with palbociclib, ribociclib, and abemaciclib: Similarities and differences. *Drugs*, 2021, 81(3), 317-331. http://dx.doi.org/10.1007/s40265-020-01461-2 PMID: 33369721
- [75] Tolaney, S.M.; Beeram, M.; Beck, J.T.; Conlin, A.; Dees, E.C.; Puhalla, S.L.; Rexer, B.N.; Burris, H.A.; Jhaveri, K.; Helsten, T.; Becerra, C.; Kalinsky, K.; Moore, K.N.; Manuel, A.M.; Lithio, A.; Price, G.L.; Chapman, S.C.; Litchfield, L.M.; Goetz, M.P. Abemaciclib in combination with endocrine therapy for patients with hormone receptor-positive, HER2-negative metastatic breast cancer: A phase 1b study. Front Oncol., 2022, 11, 810023. http://dx.doi.org/10.3389/fonc.2021.810023 PMID: 35223458
- [76] Johnston, S.R.D.; Toi, M.; O'Shaughnessy, J.; Rastogi, P.; Campone, M.; Neven, P.; Huang, C.S.; Huober, J.; Jaliffe, G.G.; Cicin, I.; Tolaney, S.M.; Goetz, M.P.; Rugo, H.S.; Senkus, E.; Testa, L.; Del Mastro, L.; Shimizu, C.; Wei, R.; Shahir, A.; Munoz, M.; San Antonio, B.; André, V.; Harbeck, N.; Martin, M. Abemaciclib plus endocrine therapy for hormone receptor-positive, HER2-negative, node-positive, high-risk early breast cancer (monarchE): Results from a preplanned interim analysis of a randomised, open-label, phase 3 trial. *Lancet Oncol.*, 2023, 24(1), 77-90. http://dx.doi.org/10.1016/S1470-2045(22)00694-5 PMID: 36493792

DISCLAIMER: The above article has been published, as is, ahead-of-print, to provide early visibility but is not the final version. Major publication processes like copyediting, proofing, typesetting and further review are still to be done and may lead to changes in the final published version, if it is eventually published. All legal disclaimers that apply to the final published article also apply to this ahead-of-print version.